Short Communication

Growth of Well-aligned Ag-doped ZnO Nanorods Arrays on FTO Substrate Using Electrochemical Approach: Optical Properties and Photocatalytic Activity

Li-li Wang*, Wei Ma, Ji-long Ma, Guo-quan Shao

Bozhou University, Bozhou Anhui 236800, China
*E-mail: llwang_89@163.com, llwang@mail.ustc.edu.cn

A simple electrochemical synthesis was successfully used for the growth of Ag-doped ZnO nanorods on fluorine-doped tin oxide to investigate the photocatalytic degradation activity. Photoluminescence (PL) spectroscopy and UV–Vis absorbance spectra at normal atmospheric conditions were used to examine the optical characteristics of the nanorods. Composition and morphology were investigated using energy-dispersive X-ray spectroscopy (EDX) and field emission scanning electron microscopy (FESEM). FESEM images show the synthesized Ag-doped ZnO nanostructures possess very high-density rod-shaped morphologies. UV-visible spectroscopy indicates a red shift in absorption peaks centered at 376 nm for Ag-doped ZnO nanorods in comparison to undoped ZnO nanorods. Pl results reveal that initially as the Ag doping is done, the vision emission intensity decreases. Photocatalytic analysis of the samples shows the degradation rate increases by doping Ag ions into ZnO lattice structures which show much higher photocatalytic degradation rates.

1. INTRODUCTION

For decades, Semiconductors have been a significant topic for research in various applications. Some of them include nanocomposites made of semiconductors along with dielectrics, polymer or another semiconductor, doped and co-doped semiconductor nanocrystals and so on. Another topic under frequent investigation is semiconductor photocatalysts under irradiation which includes metal oxides like ZnO, SnO2 and TiO2 [1-3]. ZnO with a wide band gap (3.37 eV), tops among them as a futuristic choice for Organic pollutant degradation as it is low in cost, friendly to the environment.

The photocatalytic efficiency is affected by a disadvantage of ZnO, the rapid recombination of photoexcited hole and electron pairs. To overcome this disadvantage, the recombination rate of the pair

must be slowed down and the surface charge transfer must be improved. A number of methods have been devised to alter these and one of them is doping the ZnO photocatalysts with a transition metal, which can result in alteration of electrical, magnetic and optic properties of ZnO. It also results in decreased band gap energy, the formation of electron traps to increase the charge separation and better photo catalysis activity of ZnO. Doping of ZnO is widely done by either using transition metals such as Ni, Mn, Fe, Cu, and Ag [4-6]. This enables the formation of electron traps that decrease the pair recombination rate. It has been found that doping is an effective process in the photocatalytic activities only when added in optimum concentrations. Not all metal ions resulted in progression, some decreased the photocatalytic activity by increasing the electron-hole recombination rate due to the formation of centres for recombination by making use of some of the photo induced electrons by multivalent metal ions.

RF magnetron sputtering [7], chemical vapor deposition [8], sol-gel method [9], spray pyrolysis [10], and DC magnetron sputtering [11] are some of the several techniques used to dope ZnO. But these techniques need a harsh reaction environment, which is expensive. Their selectivity to impurities is also low. However, the electrochemical preparation of ZnO on the ZnO seed layer using thermal decomposition procedure of zinc acetate is a simple, cheap, easily controllable process that uses readily available raw materials and has high selectivity to impurities. These advantages make this technology highly suitable for producing ZnO nanorods. However, studies on the synthesis of Ag-doped ZnO nanorods by the electrochemical process have not been published yet.

This current work reports the preparation and characterization of Ag-doped ZnO nanorods. Further focuses on the photocatalytic and optical properties of Ag-doped ZnO nanorods.

2. MATERIALS AND METHOD

In a typical electrochemical process, 0.1M zinc nitrate hexahydrate ($Zn(NO_3)_2.6H_2O$) and 0.05M silver nitrate ($AgNO_3$) were added to DI water and subjected to 30 min vigorous stirring. 0.1M hexamethylenetetramine (HMTA) is dissolved in 25 ml DI water and then was added to the previous solution. The resultant was subjected to 30 min stirring. A few drops of ammonium hydroxide (NH_4OH) were added to adjust the pH to 10. A homogenous mixture was made by stirring it for 20 min. The aqueous solution (25 mM) was put into a galvanic cell. The anode, platinum electrode, and the cathode, ZnO seed layer coated on fluorine-doped tin oxide (FTO) films, were placed inside the solution. Vertically aligned nano tapered ZnO structures were produced with 1 mA/cm^2 current density, 1-hour growth time and 80 °C growth temperature. DI water and nitrogen gas were used to wash and dry the sample respectively after growing the nanostructures. The samples were characterized by Field Emission Scanning Electron Microscopy (FE-SEM, FEI Sirion 200) attached with energy dispersive X-ray spectroscopy (EDX) for elemental analysis. The optical properties were investigated by photoluminescence (PL) spectroscopy (Horiba Jobin Yvon Inc. Edison, NJ, USA) at room temperature. The UV–Vis absorbance spectra were conducted with a UV-Vis Spectrophotometer (Shimadzu UV-2600). Electrochemical impedance spectroscopy (EIS) was used to examine the charge transfer and recombination processes with a potential of 10 mV at frequencies range from 0.1 Hz to 0.1MHz. In

typical measurement, Ag-doped ZnO nanorods grown on FTO substrates were used as the working electrodes. A Ag/AgCl and platinum wire were used as the reference and counter electrodes, respectively. 0.1 M Na_2SO_4 aqueous solution was used as the electrolyte in this experiment. The photocatalytic performance of Ag-doped ZnO nanorods was assessed by the degradation of methylene blue (MB) dye under UV irradiation. The photocatalytic activities of Ag ions doped ZnO nanorods were evaluated by MB, a basic aniline dye. The evaluation of the nanorods was done under UV light (>254 nm).

3. RESULTS AND DISCUSSION

FESEM was used to characterize and examine the synthesized Ag-doped ZnO samples. As shown in Figure 1, the diameters of ZnO nanorods had increased when Ag ions doped in ZnO structures. It can be seen that the morphology of the synthesized undoped and Ag-doped ZnO nanomaterials are very high-density rod-shaped structures, from the FESEM images, that these structures are made of high width to height ratio Ag-doped ZnO nanorods. The typical length and width of these Ag-doped ZnO nanorods are approximately 2 µm and 150 nm, respectively. As OH^- ions are corrosive, at higher concentrations, amphoteric ZnO undergoes partial hydrolysis [12].
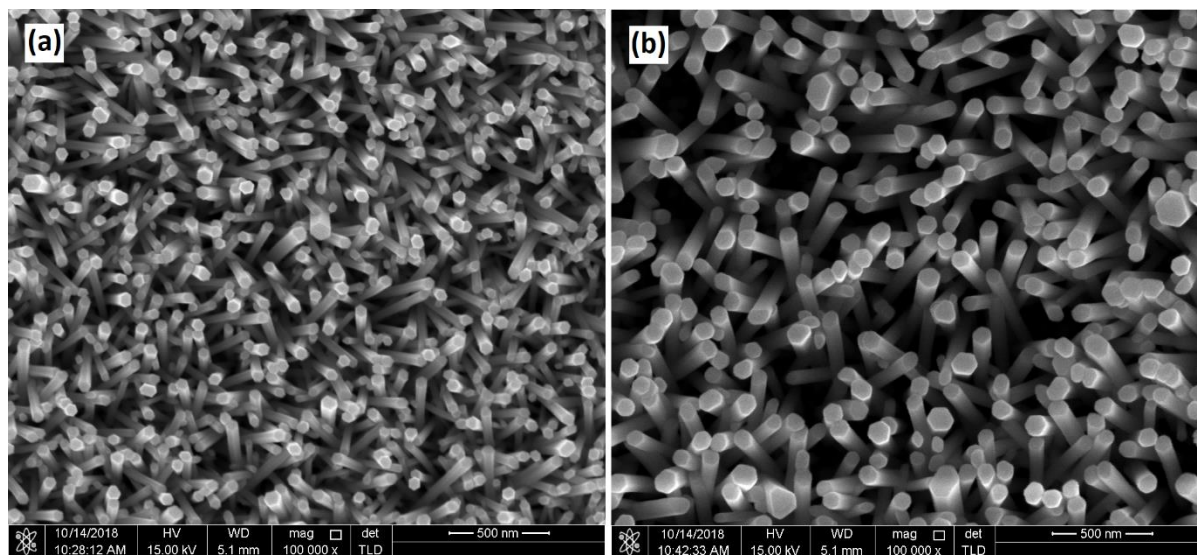

Figure 1. FESEM images of (a) undoped and (b) Ag-doped ZnO nanorods grown on FTO glass using electrochemical method at 1 mA/cm^2 current density and 80 °C growth temperature.

Thus, as reported, the synthesis of dense homogenous ZnO structures with a high aspect ratio is effective when done by electrochemical method, which holds good for photocatalytic applications that have high sensitivity and selectivity.

Energy dispersive X-ray spectroscopy (EDX) attached with FESEM was used in order to determine the elements present and the purity of synthesized rod-shaped Ag-doped ZnO nanostructures.

Fig 2 clearly shows that the synthesized nanorods consist only of Zn, Ag, and O, proving that Ag-doped ZnO nanostructures do not have any impurities or contaminations. It also denotes that they are pure.
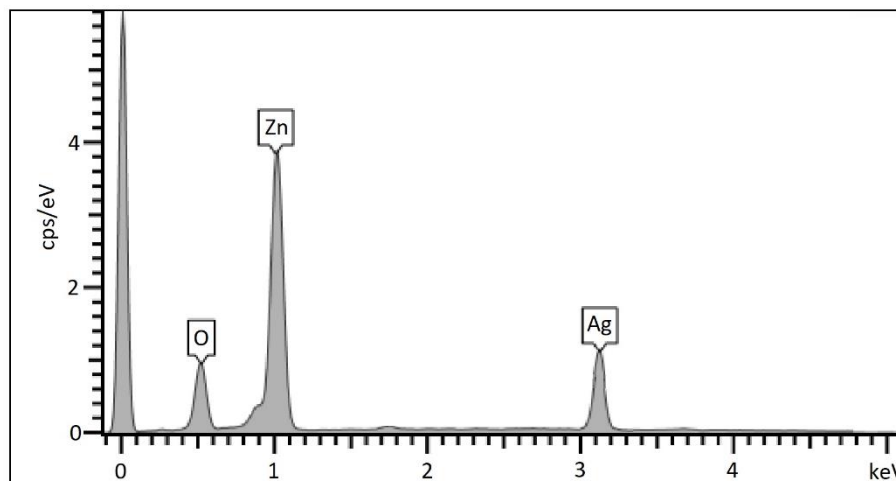

Figure 2. EDX analysis of Ag-doped ZnO nanorods grown on FTO glass using electrochemical method at 1 mA/cm^2 current density and 80 °C growth temperature.

UV-visible spectroscopy was used to study the changes in the optical properties of the nanorods when Ag was doped. The UV-visible absorption spectra of undoped and Ag-doped ZnO nanorods are shown in Fig 5. The undoped and Ag-doped ZnO nanorods exhibit band gap absorption peak centered at 374 nm (3.31 eV) (related to Wurtzite ZnO crystal) and 376 nm (3.29 eV) respectively. It is clear that the peak has undergone red shifting for doped nanorods, which can be explained by quantum size effects. This phenomenon can be observed in the FESEM images where the diameter of nanorods increase with Ag doping. This is further supported by the literature in which it is clear that the doping of Ag ions into Zn sites of ZnO nanorods will cause the absorption peak in the typical band gap to have a redshift [13].
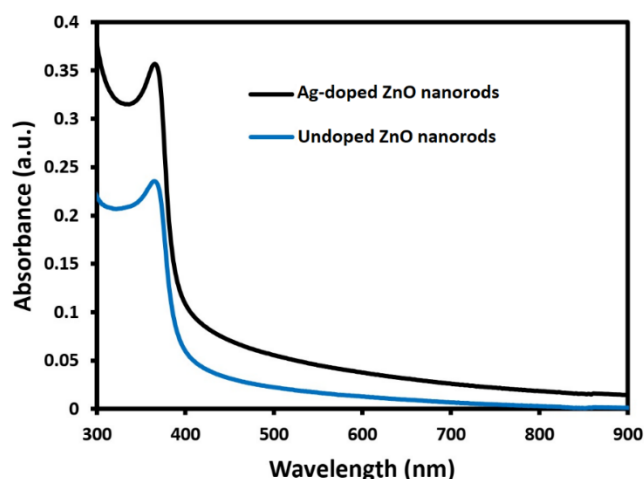

Figure 3. Optical absorption of undoped and Ag-doped ZnO nanorods grown on FTO glass using electrochemical method at 1 mA/cm^2 current density and 80 °C growth temperature.

Fig. 4 represents the PL spectra of the undoped and doped samples at normal atmospheric conditions. An intense narrow emission band is centered at 380 nm in the UV spectral range for both types of samples. These emissions generally refer to the free excitonic recombination in ZnO [14]. No change can be seen in the UV band position for doped samples. Another wide emission band is seen at the visible range centered at 580 nm. Several intrinsic and extrinsic defects are referred to cause these multicomponent visible emissions in ZnO. As shown in Fig 4, It can be easily understood that the visible emission intensity decreases as the doping of Ag into the nanorods occur. The substitution of Zn ions and Interstitial forming are the two ways in which Ag^+ ions can be added or doped into the ZnO nanostructures. Most of the Ag+ ions had been added through substitution because as the number of Ag ions added through substitution increased, more lattice defects were formed. This is clearly understood by the fact that the number of defects increase as Ag concentration increase.
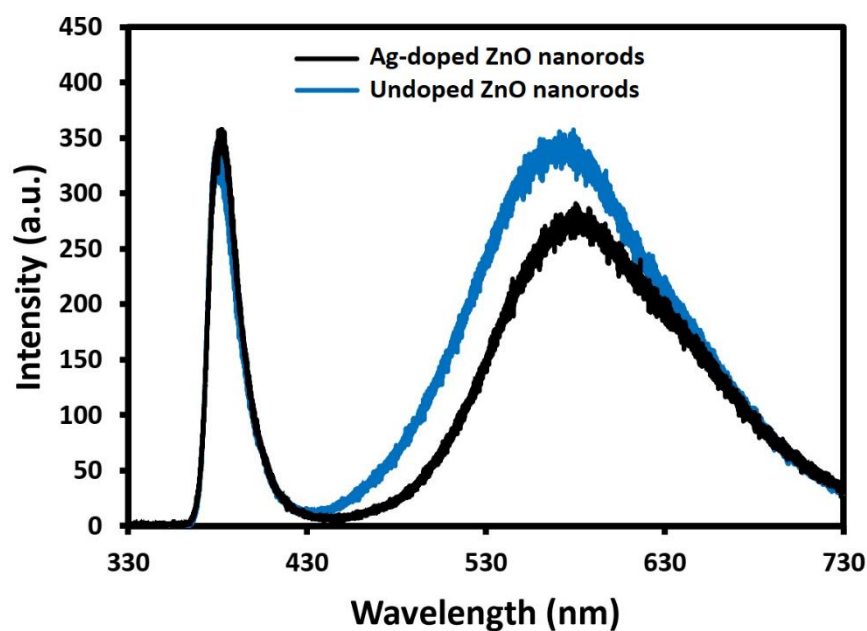

Figure 4. PL spectrum of undoped and Ag-doped ZnO nanorods grown on FTO glass using electrochemical method at 1 mA/cm² current density and 80 °C growth temperature.

Diffuse-reflectance measurements were done in the UV–vis region at room temperature to calculate the energy gap by studying the interaction of electrons that were present closer to the optical band. The band gap of transition metals ion-doped ZnO specimens were determined from the diffuse-reflectance spectra using a Kubelka–Munk function by the following equation [15]:

$$F(R)=(1-R)^2/2R \tag{1}$$

where R is the detected reflectance in UV-vis spectra, ν is the light frequency and h is Planck's constant. The band gap energy is represented by the intercept formed by the graph plotted between $[F(R)h\nu]^2$ and hν (Fig. 5). The estimated band-gaps in the visible spectrum are found to be 3.19 and 3.13

eV for undoped ZnO and Ag-doped ZnO nanorods respectively. This change in band gap energies in the experimental results show the doping of Ag^+ ions.
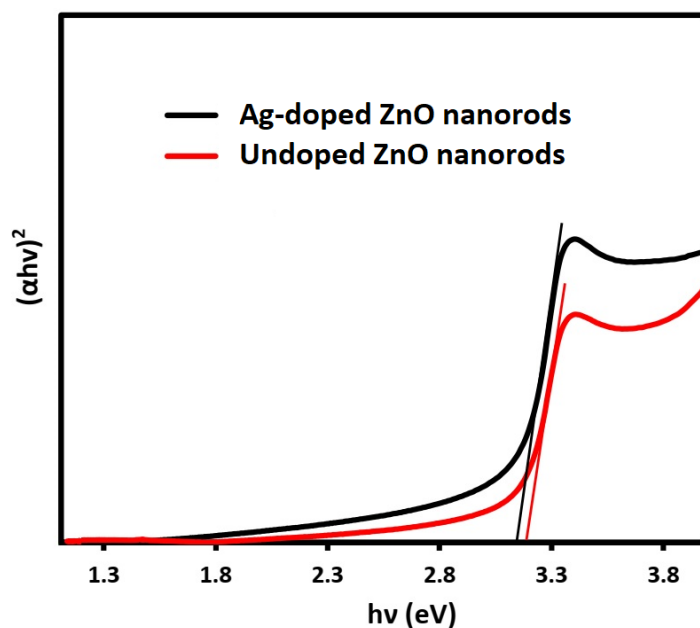

Figure 5. Ddiffuse-reflectance spectra of undoped and Ag-doped ZnO nanorods grown on FTO glass using electrochemical method at 1 mA/cm^2 current density and 80 °C growth temperature.
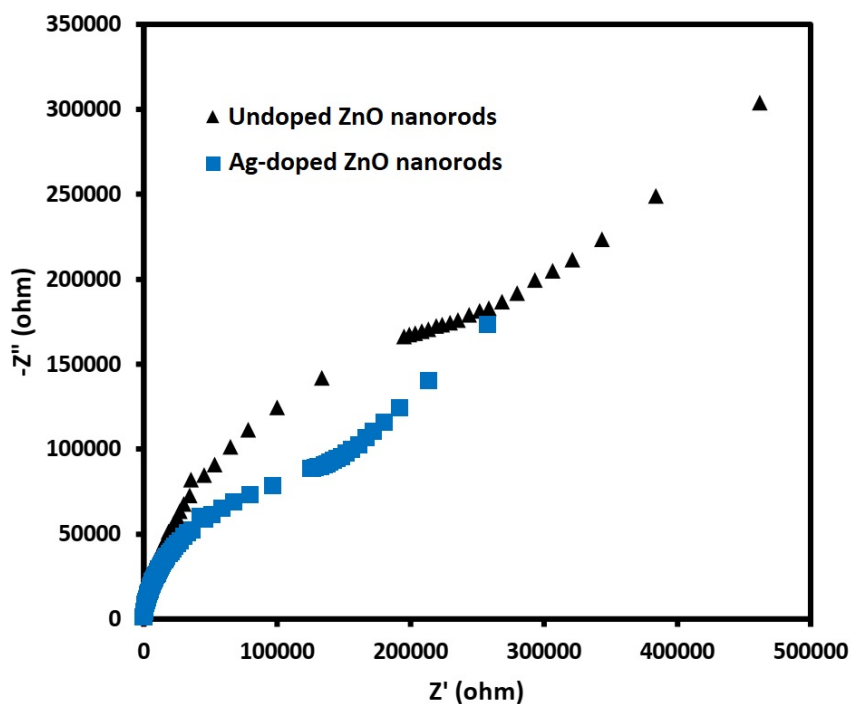

Figure 6. Nyquist plots of undoped and Ag-doped ZnO nanorods in 0.1 M Na$_2$SO$_4$ aqueous solution as electrolyte.

The interface properties and charge transfer efficiency of samples had been investigated by electrochemical impedance measurement [16]. Figure 6 shows Nyquist diagrams between a real and imaginary impedance for undoped ZnO and Ag-doped ZnO nanorods. The arc radius reveals the resistance of interface layer at the electrode surface. As the charge transfer efficiency is reduced, the radius of arc increases. The Ag ions doping decrease the resistance of the interface layer, revealing the developed interfacial charge-carrier separation and efficiency of charge transfer on the ZnO surface. These findings demonstrate that doping Ag ions in ZnO nanostructures can cause higher free-electron carriers which accelerate charge transfer and decrease the resistance, it is beneficial for the enhancement of the ZnO photocatalytic activity.

MB was selected, in the current work, as a synthetic basic dye for assessment of the Ag ions doped ZnO nanorods photocatalytic efficiency in photocatalysis [17]. The MB has been widely used to be the thotocatalytic activity index. The photocatalytic degradation rates of MB (30 mgl^{-1}) on Ag ions doped ZnO nanostructures can be seen in Fig. 7. It can be seen from Fig. 7 that the degradation rate increases by doping Ag ions into ZnO lattice structures which show higher rates of photocatalytic degradation. 95% and 100% of MB was removed in <30 min and 60 min respectively in Ag-doped ZnO nanorods. This clearly shows that the doping of Ag$^+$ ions has an improving effect on the photocatalytic degradation activities of ZnO nanorods.
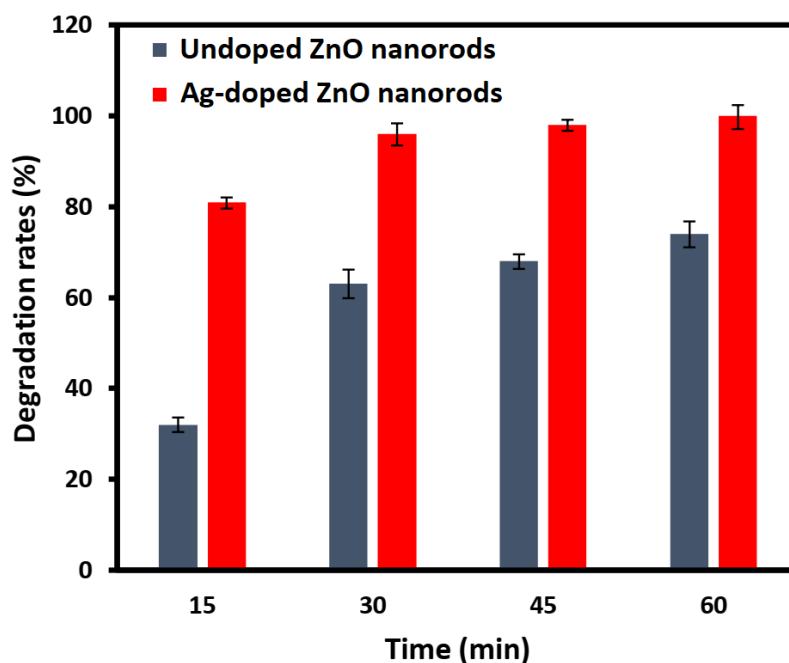

Figure 7. The degradation rates of the undoped and Ag-doped ZnO nanorods evaluated by Methylene blue dye under UV light

Table 1. Overview of the Ag-doped ZnO nanorods with their synthesis techniques and photocatalytic performances.

Dopant	Synthesis method	Pollutant	Time (min)	Deg. (%)	Ref.
Ag	Solid state milling method	Methyl violet	120	~43	[18]
Ag	Sol–gel method	Methylene blue	120	~95	[19]
Ag	borohydride reduction method	Congo Red	60	~81	[20]
Ag	Hydrothermal method	Tartrazine	90	~99	[5]
Ag	Electrochemical method	Methylene blue	60	~100	This work

The photocatalytic activity of the ZnO may decrease due to higher surface doping, which covers the surface of ZnO and prevents light absorption and pollutant adsorption. Table 1 presents Ag transition metals influence on the photodegradation of various dyes according to previous researches [5, 18-20]. In comparison with previous reported works containing Ag transition metals as doping materials, Ag-doped ZnO photocatalyst in this study has the highest photocatalytic activity under UV light. According to Table 1, Ag-doped ZnO nanorods may be a good choice for wastewater treatment.

4. CONCLUSION

Ag-doped ZnO nanorods have been synthesized at low-cost and convenient electrochemical techniques. The structural results exhibit the growth of rod-like ZnO single crystal along the vertical direction. Room temperature PL spectra showed UV emissions with center at 381 nm and broad emissions in the visible range of 465 nm to 690 nm. The sharp feature that appeared in the UV emission region indirectly shows the narrow distribution of the nanorods, which has good accordance with the FESEM results. The band-gap energies of the undoped ZnO and Ag-doped ZnO nanorods by Kubelka–Munk function are found to be 3.24 and 3.15 eV respectively, relating to the visible spectrum. These clearly show that the photocatalytic activities of Ag-doped ZnO nanorods are higher than undoped ZnO under UV light. The development of Ag-doped ZnO photocatalysts might be considered an advance in the large-scale operation of heterogeneous photocatalysis by UV radiation to address aqueous contamination.

References

1. M.R.D. Khaki, M.S. Shafeeyan, A.A.A. Raman and W.M.A.W. Daud, *Journal of Molecular Liquids*, 258 (2018) 354.
2. Y. He, N.B. Sutton, H.H. Rijnaarts and A.A. Langenhoff, *Applied Catalysis B: Environmental*, 182 (2016) 132.
3. L. Yang, J. Huang, L. Shi, L. Cao, W. Zhou, K. Chang, X. Meng, G. Liu, Y. Jie and J. Ye, *Nano Energy*, 36 (2017) 331.
4. V. Mote, Y. Purushotham and B. Dole, *Materials & Design*, 96 (2016) 99.

5.   Ş.Ş. Türkyılmaz, N. Güy and M. Özacar, *Journal of Photochemistry and Photobiology A: Chemistry*, 341 (2017) 39.
6.   A. Alhadhrami, A.S. Almalki, A.M.A. Adam and M.S. Refat, *International Journal of electrochemical Science*, 13 (2018) 6503.
7.   H.-S. Chin, L.-S. Chao and C.-C. Wu, *Materials Research Bulletin*, 79 (2016) 90.
8.   Z. Ye, T. Wang, S. Wu, X. Ji and Q. Zhang, *Journal of Alloys and Compounds*, 690 (2017) 189.
9.   R. Mohamed, J. Rouhi, M.F. Malek, A.S. Ismail, S.A. Alrokayan, H.A. Khan, Z. Khusaimi, M.H. Mamat and M.R. Mahmood, *International Journal of Electrochemical Science*, 11 (2016) 2197.
10. E. Muchuweni, T. Sathiaraj and H. Nyakotyo, *Ceramics International*, 42 (2016) 10066.
11. B.B. Sahu, J.G. Han, J.B. Kim, M. Kumar, S. Jin and M. Hori, *Plasma Processes and Polymers*, 13 (2016) 134.
12. J. Rouhi, C.R. Ooi, S. Mahmud and M.R. Mahmood, *Materials Letters*, 147 (2015) 34.
13. S. Jeong, B. Park, S.-B. Lee and J.-H. Boo, *Surface and Coatings Technology*, 201 (2007) 5318.
14. K. Eswar, J. Rouhi, H. Husairi, M. Rusop and S. Abdullah, *Advances in Materials Science and Engineering*, 2014 (2014) 1.
15. J.-i. Fujisawa, T. Eda and M. Hanaya, *Chemical Physics Letters*, 685 (2017) 23.
16. M. Husairi, J. Rouhi, K. Alvin, Z. Atikah, M. Rusop and S. Abdullah, *Semiconductor Science and Technology*, 29 (2014) 075015.
17. H. Salavati and H. Saedi, *International Journal of Electrochemical Science*, 10 (2014) 4208.
18. M. Ibănescu, V. Muşat, T. Textor, V. Badilita and B. Mahltig, *Journal of Alloys and Compounds*, 610 (2014) 244.
19. P. Amornpitoksuk, S. Suwanboon, S. Sangkanu, A. Sukhoom, N. Muensit and J. Baltrusaitis, *Powder Technology*, 219 (2012) 158.
20. N. Güy and M. Özacar, *International Journal of Hydrogen Energy*, 41 (2016) 20100.